Eur. Phys. J. A **21**, 383–390 (2004)
DOI 10.1140/epja/i2004-10009-9

THE EUROPEAN PHYSICAL JOURNAL A

Excited states in ^{163,164}Ho populated through incomplete-fusion reactions

D. Hojman[1,2,a], M.A. Cardona[1,2,3], D. Bazzacco[4], N. Blasi[5], J. Davidson[1,2], M. Davidson[1,2], M.E. Debray[1,3], A.J. Kreiner[1,2,3], S.M. Lenzi[4], G. Lo Bianco[6], D.R. Napoli[7], and C. Rossi Alvarez[4]

[1] Departamento de Física, Comisión Nacional de Energía Atómica, Buenos Aires, Argentina
[2] CONICET, Buenos Aires, Argentina
[3] Escuela de Ciencia y Tecnología, Universidad de San Martín, San Martín, Argentina
[4] Dipartimento di Fisica, Sezione di Padova, Padova, Italy
[5] Dipartimento di Fisica and INFN, Sezione di Milano, Milano, Italy
[6] Dipartimento di Fisica, Università di Camerino, Camerino (Perugia), Italy
[7] INFN, Laboratori Nazionali di Legnaro, Legnaro (Padova), Italy

Received: 13 February 2004 / Revised version: 18 March 2004 /
Published online: 14 September 2004 –
Communicated by D. Schwalm

Abstract. High-spin states in ^{163,164}Ho were investigated by means of in-beam γ-ray spectroscopy techniques using the multidetector array GASP. Excited states in ^{163,164}Ho were populated predominantly through the incomplete-fusion mechanism in the ^{160}Gd(^{11}B, αxn) reaction at a beam energy of 61 MeV. Known rotational bands in ^{163}Ho have been extended to higher spins and a three-quasiparticle band has been observed in this nucleus. Rotational bands have been identified in ^{164}Ho and their configurations have been discussed. Empirical Gallagher-Moszkowski (GM) splitting energies were extracted from the $\pi 7/2^-[523] \otimes \nu 5/2^-[523]$ and $\pi 7/2^-[523] \otimes \nu 5/2^+[642]$ GM doublets. Alignments, band crossing frequencies, and electromagnetic properties have been analyzed in the framework of the cranking model.

PACS. 21.10.Re Collective levels – 21.60.Ev Collective models – 23.20.Lv γ transitions and level energies – 27.70.+q $150 \leq A \leq 189$

1 Introduction

The decay of high-spin states of nuclei populated in heavy-ion–induced reactions and observed in γ-ray spectroscopy studies, provides an important tool for the investigations on nuclear structure. Powerful instruments, such as GASP [1], make it possible to observe not only bands belonging to the strongly populated residual nuclei, but also cascades of γ-rays produced in the de-excitation of sometimes weak reaction channels. Here, we present the rotational band structures of ^{163,164}Ho populated basically through the incomplete-fusion mechanism in the bombardment of ^{160}Gd with a beam of 61 MeV ^{11}B ions. These results were obtained from measurements focused on the study of ^{166}Tm through the ^{160}Gd(^{11}B, $5n$) reaction [2]. Until now, the spectroscopy studies of ^{163,164}Ho were performed using light-projectile reactions. Very recently, Jungclaus *et al.* [3] reported the population of ^{163}Ho via the ^{160}Gd(^{7}Li, $4n$) reaction. For the production of ^{164}Ho the reaction ^{160}Gd(^{7}Li, $3n$) is not suitable, because the optimum energy is at about 30 MeV, very close to the Coulomb barrier, then in this case the incomplete-fusion reactions become a good alternative. Incomplete-fusion reactions have recently been used in the study of nuclei close to the stability zone, as a mean to populate high-spin states with rather large yields and construct level schemes using in-beam γ-ray spectroscopy techniques [3,4]. These nuclei were commonly studied through light-projectile–induced reactions, and the spectrum measurements of the outgoing particles were often used to establish excited levels and their configuration assignments.

The nuclear structure at low excitation energy in ^{163}Ho is well established from radioactive decay and in-beam γ-ray experiments using the $(d, 2n)$ and the (p, n) reactions [5] as well as from the (^{3}He, d), (α, t), and (t, α) reaction studies [6,7]. In the case of ^{164}Ho, its level structure was deduced from the analysis of the particle spectra in the (d, t) [8] and the (γ, n) [9] reactions. Prior to this work, limited experimental data of γ-rays of ^{164}Ho were available. Since ^{164}Ho has stable isobaric neighbors the levels of this nucleus are not accessible through β-decay. Early γ-ray measurements were performed using

[a] e-mail: hojman@tandar.cnea.gov.ar

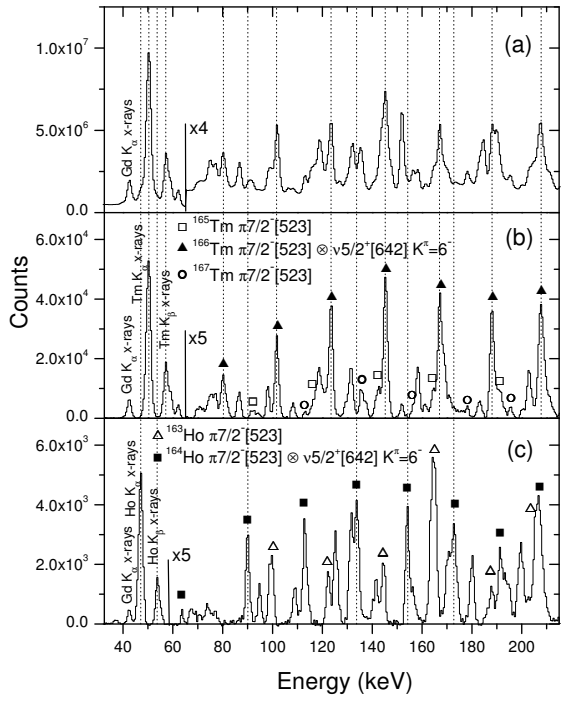

Fig. 1. γ-ray spectra of Ge detectors obtained from the symmetric cube analysis corresponding to (a) total projection, (b) double gate on Tm K_α X-rays, (c) double gate on Ho K_α X-rays.

the ^{164}Dy$(d, 2n)$ and ^{164}Dy(p, n) [10,11], and the ^{165}Ho$(n, 2n)$ [12] reactions and provided information on γ-ray cascades below ≈ 600 keV.

2 Experimental procedure and data sorting

High-spin states in ^{163,164}Ho were populated through the ^{160}Gd$(^{11}$B$, \alpha xn)$ reaction at a beam energy of 61 MeV. The beam was provided by the Tandem XTU accelerator of Legnaro and was focused on a stack of three foils. Each foil consisted of 180 μg/cm^2 isotopically enriched ^{160}Gd$_2$O$_3$ evaporated onto a 15 μg/cm^2 carbon layer. The γ-rays emitted in the reaction were detected using the GASP array, consisting of 40 Compton-suppressed large-volume Ge detectors, and a multiplicity filter of 80 BGO elements, providing the sum energy and γ-ray multiplicity. Events were collected when at least 3 suppressed Ge and 3 inner multiplicity filter detectors fired. With this condition a total of 10^9 events was recorded. The data corresponding to Ge energies were sorted into a fully symmetrized cube gated by an energy-dependent window in the Ge times with respect to the BGO trigger. This gate excluded delayed events proceeding from neutron-induced reactions without loss of efficiency at low energy where the events are delayed due to their slower collection times. The total projection of this cube, in the low-energy range, is shown in fig. 1(a). The cross-section of the ^{11}B on ^{160}Gd reaction is dominated by the neutron evaporation channels (leading to the Tm isotopes) as is apparent from the large peaks of Tm X-rays observed in fig. 1(a). The Ho K_α X-rays are also clearly seen in fig. 1(a), (bump in the left of the Tm K_α X-rays) giving an indication of possible processes in which an α-particle and some neutrons appear in the exit channel together with a Ho isotope. Double gates were set on Tm K_α X-rays (fig. 1(b)) and on Ho K_α X-rays (fig. 1(c)). In these latter spectra the X-ray coincidence condition enhanced the cascades which contain strong highly converted transitions in the K-shell. In fig. 1(b) lines belonging to the bands $\pi 7/2^-[523]$ of ^{165}Tm [13], $\pi 7/2^-[523] \otimes \nu 5/2^+[642]$ $K^\pi = 6^-$ of ^{166}Tm [2,14], and $\pi 7/2^-[523]$ of ^{167}Tm [15] are indicated. In fig. 1(c) coincidences with the Ho X-rays allowed the identification of transitions belonging to Ho isotopes. The ^{163}Ho and ^{164}Ho are populated with rather similar cross-sections. In fig. 1(c) lines belonging to the $\pi 7/2^-[523]$ band of ^{163}Ho [5] and to the $\pi 7/2^-[523] \otimes \nu 5/2^+[642]$ $K^\pi = 6^-$ band of ^{164}Ho (as established in the present work) are indicated. Comparing areas of Ho and Tm K_α X-rays in fig. 1(a) and the vertical scales of the spectra of figs. 1(b) and (c), a production of Ho isotopes around 10% relative to Tm isotopes can be estimated. This yield is 20 times larger than the one calculated using the statistical model code PACE2 [16] for the evaporation channels leading to Ho residues in the ^{160}Gd + ^{11}B reaction and is associated with incomplete fusion. In this latter process the ^{11}B projectile breaks up near the target nucleus into an α-particle, which escapes without interaction, and a ^{7}Li fragment, which fuses with the target, and subsequently, the evaporation of three or four neutrons leads to ^{164}Ho or ^{163}Ho, respectively. However, the populations of the residual nuclei are distinctly different from those expected in the ^{160}Gd$(^7$Li$, xn)$ reaction, in which the $3n$ channel (^{164}Ho) is largely suppressed by the effect of the Coulomb barrier, and according to the PACE2 calculations about 10 times weaker than the $4n$ channel (^{163}Ho). In addition, the incomplete-fusion reaction acts as a filter to select high-angular-momentum states, as has been pointed out in ref. [4].

3 Experimental results

The level scheme of ^{163}Ho obtained in the present work is shown in fig. 2. Bands 2, 3, and 4, previously known up to spins (23/2), (19/2), and (21/2) [5,17], were extended up to (35/2), (31/2), and (41/2), respectively. Representative double-gated coincidence spectra are shown in figs. 3(a) and (b). In fig. 3(b) transitions of bands 3 and 4 and some interband lines are indicated. Band 1 was assigned to ^{163}Ho on the basis of coincidence relationships with members of the already known band 2. Its bandhead was established as $(17/2^+)$ after considering the configuration of the band, as discussed below. In fig. 3(a) lines belonging to bands 1 and 2 are indicated and in the inset the 973.1 keV decay transition is clearly seen. In our first sorting of the data, the detectors at different angles were Doppler shifted by using prompt γ-rays as is usually done in the thin-target experiments. With this correction, the detected peaks which have lifetimes longer

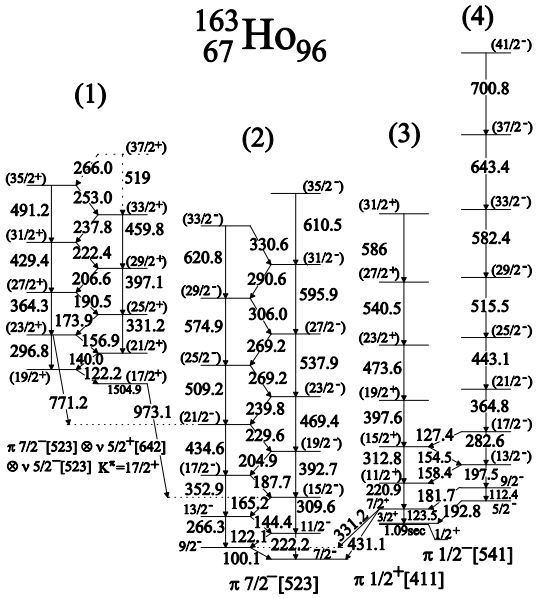

Fig. 2. Level scheme of ^{163}Ho proposed in the present work. The $1/2^+$ state of band 3 and its half-life are from ref. [17].

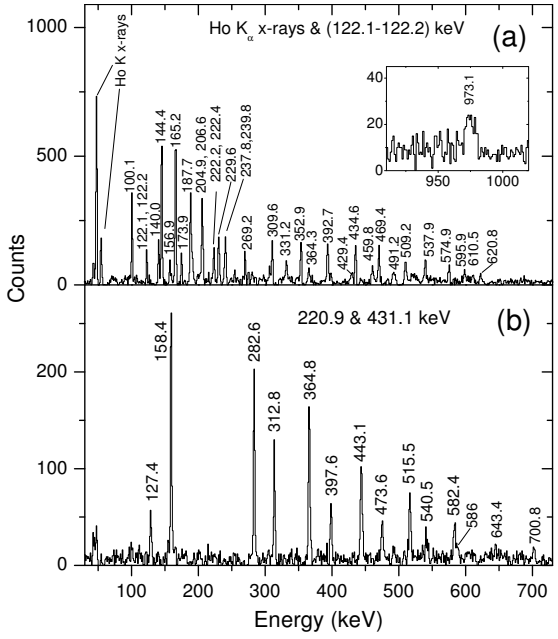

Fig. 3. γ-ray coincidence spectra of Ge detectors obtained setting double gates on: (a) Ho K_α X-rays and the 122.1–122.2 keV doublet observed in ^{163}Ho. In the inset the 973.1 keV line has been obtained without Doppler correction; (b) 220.9 and 431.1 keV transitions of ^{163}Ho.

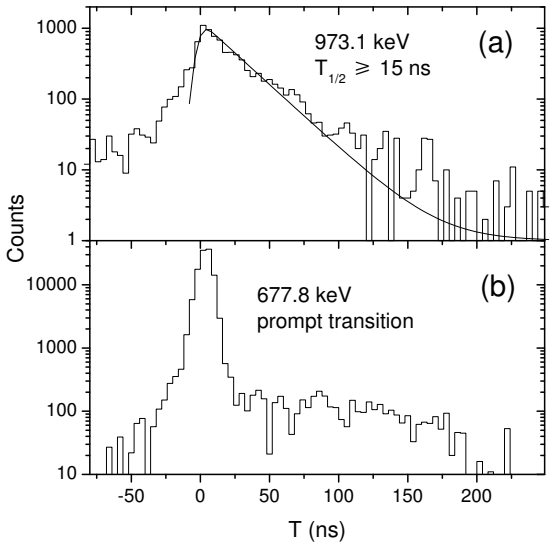

Fig. 4. Time spectra corresponding to the (a) 973.1 keV (delayed), (b) 677.8 keV (prompt) transitions. In part (a) the fit of the data using an exponential decay folded with a Gaussian function is shown. For a better selection of the lines of interest, coincidences with Ho and Tm K_α X-rays were required for the 973.1 and 677.8 keV time distributions, respectively.

than the slowing-down time of the nuclei in the target material, and which are therefore predominantly emitted from stopped nuclei in the successive target foils, are not correctly matched and consequently appear widened; this was the situation for the 973.1 keV line. Another sorting of the data without Doppler correction was performed and a normal width was obtained for the 973.1 keV peak (inset of fig. 3(a)). Figures 4(a) and (b) show the time distributions with respect to the BGO filter of the 973.1 keV line and, for comparison, of the 677.8 keV prompt transition belonging to the yrast band of ^{166}Tm, respectively. From these figures the isomeric character of the 973.1 keV line is clearly seen. Since a fraction of the residual nuclei is not stopped in the target, and consequently flies away and, depending on the half-life, can decay out of the detection system, only a lower limit, $T_{1/2} \geq 15$ ns, was obtained for the half-life of the $(17/2^+)$ state of band 1.

The level scheme of ^{164}Ho proposed in the present work is shown in fig. 5. The identification of γ-rays belonging to ^{164}Ho was based on coincidences with Ho X-rays, the knowledge of the neighboring ^{163}Ho ([5], and this work), ^{165}Ho [13] (weakly populated in this experiment) nuclei, and transitions and coincidence data reported in refs. [10,11]. The excited levels and their configuration assignments established in ref. [8] were also used in the construction of the level scheme. Examples of double-gated coincidence spectra displaying lines of bands 1–5 are shown in figs. 6(a)-(e). The 63.9 keV line and the 90.1-112.7-133.7 keV cascade were reported in ref. [10] as belonging to ^{164}Ho. In the present work we identified these lines as the first $\Delta I = 1$ transitions of the yrast band labeled as band 2 in fig. 5. In the case of band 3, the 202.8-109.6-127.3-143.6 keV cascade was reported in ref. [10] and the first three states of this band were strongly populated in the ^{165}Ho(d,t) reaction [8]. In the present work we extended band 3 up to spin (12). The first two 37.3 and 56.7 keV $\Delta I = 1$ transitions of band 4 were observed in the decay of the 6^- isomer (bandhead of band 2), through the 45.9 keV $E3$ transition and identified as members of the ground-state band [12,18]. We

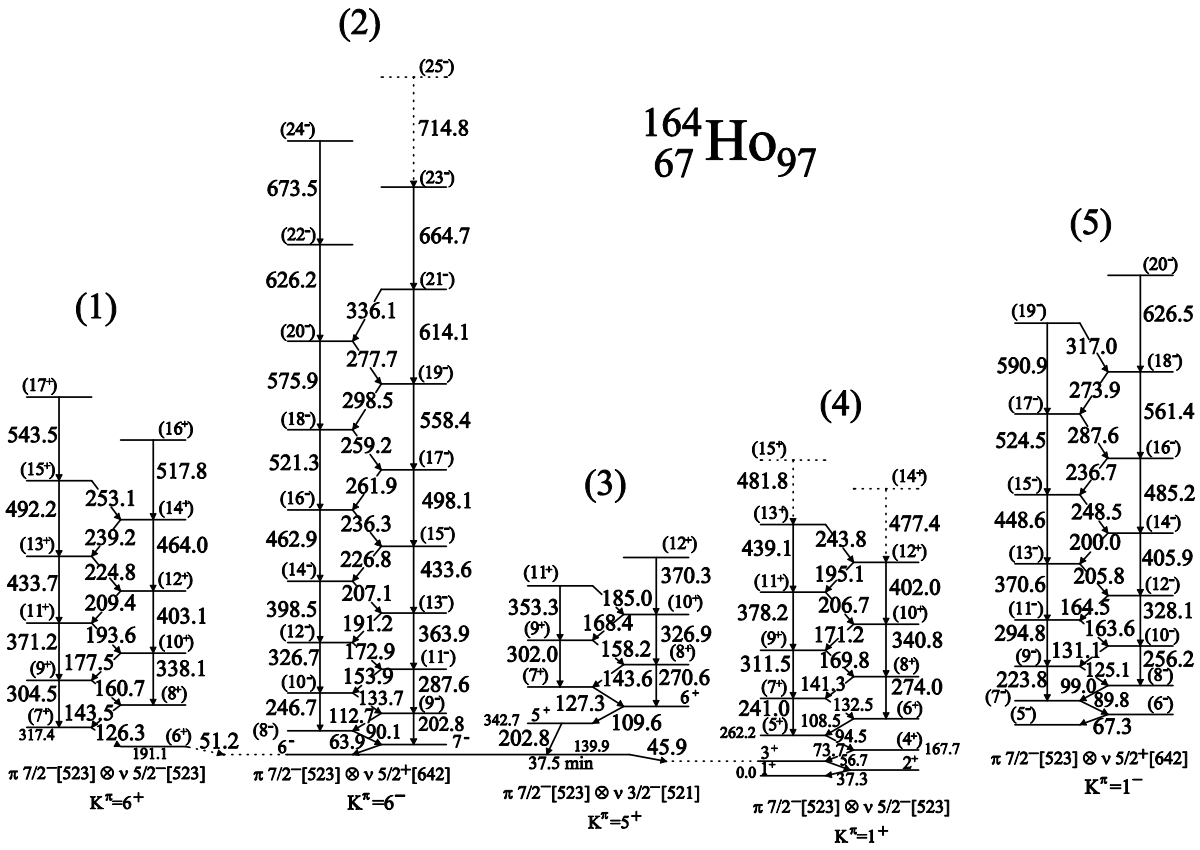

Fig. 5. Level scheme of ^{164}Ho proposed in the present work. The decay of the 6^- isomer through the 45.9 keV $E3$ transition and its half-life are from ref. [18].

extended this band up to an excitation energy of about 2 MeV. The placements of the 73.7 and 94.5 keV transitions in band 4 which establish the (4^+) and (5^+) states at 167.7 and 262.2 keV, respectively, are supported by coincidence relationships and similarities with the equivalent structure observed in ^{162}Ho which contains the sequence of 38.3, 57.8, 75.6, and 99.6 keV lines [19]. In addition, the 167.7 (4^+) and 262.2 keV (5^+) levels are in close energy agreement with those assigned in ref. [8] as the 4^+ and 5^+ members of the ground-state band. Transitions of band 5 are reported in this work for the first time. The assignment of band 5 to ^{164}Ho is supported by the coincidences of lines of this band with the out-of-band 156.0, 193.3, 198.8, and 208.0 keV transitions identified in ^{164}Ho [10,11]. We propose for the low-lying levels of band 5 and its decay the scheme shown in fig. 7, based on the following arguments: a) The 113.6, 156.0, 170.6, 179.8, 193.3, 198.8, and 208.0 keV transitions are in coincidence with the lines of band 5 but not among them. In addition, the placements of the 156.0, 193.3 and 198.8 keV lines agree with those presented in ref. [10]. b) Energy sum loops are satisfied within the experimental errors. c) There is evidence of a 37.3-37.7 keV double peak, as was verified by a double-gated spectrum on Ho K_α X-rays and on the 37.3-37.7 keV doublet which displayed the same doublet. The second member of the doublet was placed in band 5. In addition, among all the decay lines the 198.8 keV γ-ray displays the strongest coincidence with the 37.3-37.7 keV doublet as is expected according to its placement in the decay scheme (fig. 7). d) The double-gated spectrum on the 163.6 and 164.5 keV lines of band 5 displays another peak at 163.5 keV and a peak at 73.7 keV. e) The resulting 236.1 keV (3^-) level agrees with that known from the particle transfer work and proposed as the (3^-) state of the $\pi 7/2^-[523] \otimes \nu 5/2^+[642]$ $K^\pi = 1^-$ structure [8]. We also assigned this structure to band 5 (see below). Thus, the decaying lines from band 5 into band 4 ($\pi 7/2^-[523] \otimes \nu 5/2^-[523]$ $K^\pi = 1^+$) correspond to neutron $E1$, $\Delta K = 0$ transitions. In coincidence spectra gated on lines of band 5 the strongest decays correspond to the $[(4^-) \rightarrow 3^+]$ 179.8, $[(3^-) \rightarrow 2^+]$ 198.8, $[(2^-) \rightarrow 1^+]$ 208.0, and $[(1^-) \rightarrow 1^+]$ 193.3 keV transitions, in this order of decreasing intensity. Delayed components were reported for the 156.0, 193.3, 198.8, and 208.0 keV transitions with half-lives of about 10 ns [11]. Assuming this value for the half-life of the bandhead of band 5, hindrance factors relative to the Weisskopf estimate $F_{\rm W}^{E1} \approx 10^5$–$10^6$ were obtained for the 156.0 and 193.3 keV transitions, which fall within the systematics for an $E1$, $\Delta K = 0$ transition [20]. Finally, another band (labeled as band 1 in fig. 5) was

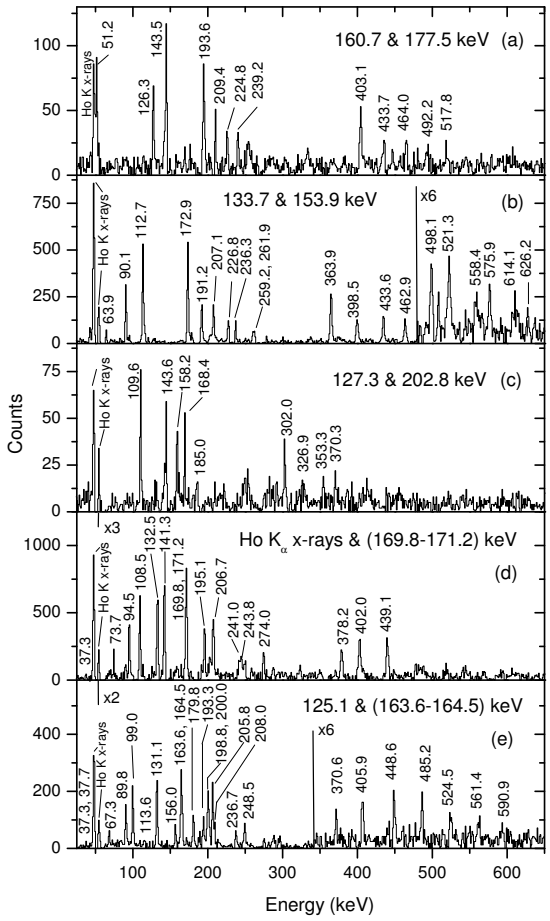

Fig. 6. Double-gated spectra displaying lines of bands of ^{164}Ho obtained setting gates on: (a) transitions of band 1 (160.7 and 177.5 keV), (b) transitions of band 2 (133.7 and 153.9 keV), (c) the 127.3 keV line of band 3 and the 202.8 keV decay transition, (d) Ho K_α X-rays and the 169.8-171.2 keV doublet observed in band 4, (e) 125.1 and the 163.6-164.5 keV doublet of band 5.

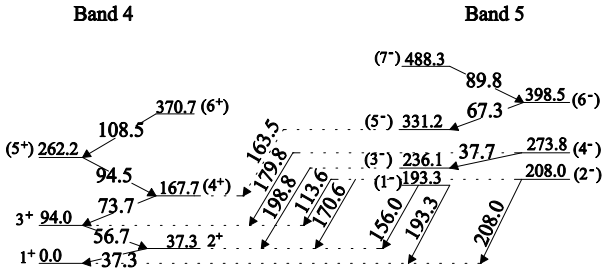

Fig. 7. Proposed decay of band 5 into band 4 in ^{164}Ho.

observed in coincidence with Ho K_α X-rays. The first 126.3 keV $\Delta I = 1$ transition is in very good agreement with the energy difference of the 318 keV 7^+ and the 191 keV 6^+ states of the $\pi 7/2^-[523] \otimes \nu 5/2^-[523]$ $K^\pi = 6^+$ band reported in ref. [8]. In addition, a 51.2 keV line is observed in coincidence with the 160.7 and 177.5 keV lines of band 1 (fig. 6(a)), which can be assumed as the transition linking the 191.1 keV (6^+) bandhead and the 139.9 keV 6^- bandhead of band 2. The absence of observed coincidences with lines of other bands of ^{164}Ho forbade an unambiguously assignment of band 1 to this nucleus.

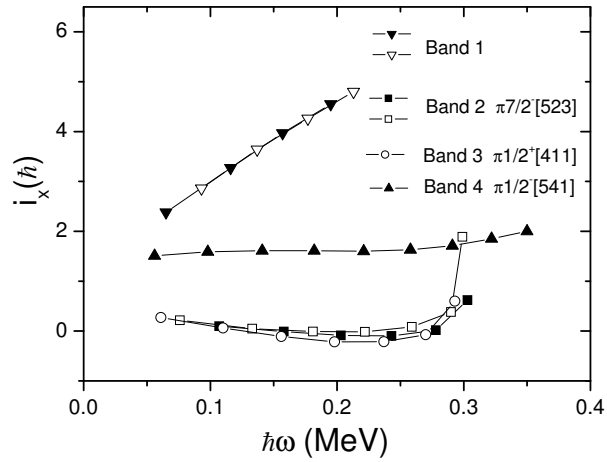

Fig. 8. Aligned angular momenta relative to the reference configuration *versus* rotational frequency for the bands of ^{163}Ho. The Harris parameters, $J_0 = 44\hbar^2/\,\mathrm{MeV}$ and $J_1 = 60\hbar^4/\,\mathrm{MeV}^3$, were used for the reference configuration. Filled and open symbols correspond to the $\alpha = +1/2$ and $\alpha = -1/2$ signatures, respectively.

4 Discussion

4.1 The ^{163}Ho nucleus

We identified band 1 as a three-quasiparticle band and assigned the configuration $\pi 7/2^-[523] \otimes \nu 5/2^+[642] \otimes \nu 5/2^-[523]$ $K^\pi = 17/2^+$ mainly on the basis of similarities with the same structure identified in the neighboring isotone ^{165}Tm [21]. In fact in both isotones the mentioned band presents the following characteristics: a) bandhead at around 1.5 MeV above the $7/2^-$ state of the $\pi 7/2^-[523]$ band. b) Decay into the $\pi 7/2^-[523]$ band through 0.8–1 MeV transitions. c) Large alignment at low frequency, consistent with the presence of the neutron $i_{13/2}$, and a gradual upbend (fig. 8). d) Strong $\Delta I = 1$ in-band transitions which compete successfully with the collective $E2$ transitions, for the ^{165}Tm band values of $B(M1)/B(E2) \approx 0.8\ \mu_N^2/e^2b^2$ have been reported. In the present work, the low statistics and the presence of contaminants did not allow the measurement of branching ratios from spectra gated on transitions above the level of interest needed to determine the $B(M1)/B(E2)$ ratios. However, an evaluation of this value, $B(M1)/B(E2) \geq 0.5\ \mu_N^2/e^2b^2$, was performed using the intensity data of the 173.9 and the 331.2 keV transitions in the gated spectrum of fig. 3(a). The assignment is further supported by the excitation energy of the $\nu 5/2^+[642] \otimes \nu 5/2^-[523]$ $K^\pi = 5^-$ structures in the even-even neighbors ^{162}Dy [19] and ^{164}Er [18] at 1485.7 and 1664.2 keV, respectively. With the present assignment to band 1 the 973.1 and 771.2 keV lines are $\Delta I = 1$, $E1$ transitions. The isomeric character of the 973.1 keV is compatible with a K-forbidden $E1$

type. This type of K isomers has been observed in deformed nuclei associated with states with good quantum number K which decay through the so-called K-forbidden transitions ($\Delta K > \lambda$, λ being the transition multipolarity). These transitions are usually characterized by the hindrance factor, $F_{\rm W} = T^{\gamma}_{1/2}/T^{\rm W}_{1/2}$ or the reduced hindrance factor, $f_\nu = F_{\rm W}^{1/\nu}$, where $\nu = \Delta K - \lambda$ is the degree of K-forbiddenness, $T^{\gamma}_{1/2}$ the partial γ half-life and $T^{\rm W}_{1/2}$ the Weisskopf single-particle estimate. The typical behavior presented by Löbner [20] is that the hindrance factor increases on average by a factor of 100 per degree of K-forbiddenness ($f_\nu = 100$ and $F_{\rm W} = 1$ for $\Delta K = \lambda$); however large deviations have been observed implying changes in the purity of the K quantum numbers of the involved states [22,23]. The 973.1 keV $E1$ transition to the $K^\pi = 7/2^-$ band is four K-forbidden and has $f_\nu \geq 8.8$, the general hindrance of the $E1$ transitions is considered by multiplying $T^{\rm W}_{1/2}$ by 10^4 before calculating f_ν [24]. This value can be compared with the reduced hindrance factors for the $\Delta I = 1$, $E1$ decays of the $\nu 5/2^+[642] \otimes \nu 5/2^-[523]$ $K^\pi = 5^-$ structure bandhead to the 4^+ state of the ground-state band in the even-even neighbors ^{162}Dy [19] and ^{164}Er [18], which are $f_\nu = 7.0$ and $f_\nu < 3.4$, respectively. In ^{164}Er the small f_ν reveals that this 5^- state is not pure and involves considerable mixing of components with $K < 5$, while in ^{162}Dy a calculation performed in ref. [25] shows that a mixing of only $\approx 5 \times 10^{-3}$ of a $K = 0$ component (associated with the other member of the GM doublet) explains the hindrance of the transitions decaying into the ground-state band. On account of the hindrance factors the scenario presented in ^{163}Ho is similar to the ^{162}Dy case with a rather pure $K = 17/2$ state for the $\pi 7/2^-[523] \otimes \nu 5/2^+[642] \otimes \nu 5/2^-[523]$ bandhead.

Bands 2, 3 and 4 have been previously identified as the $\pi 7/2^-[523]$, $\pi 1/2^+[411]$, and $\pi 1/2^-[541]$ structures, respectively [5]. The aligned angular momenta, relative to the reference configuration, for these bands are plotted in fig. 8. The reference configuration was obtained by fitting I_x, the total angular momentum on the rotational axis, for the $\pi 1/2^-[541]$ structure in the frequency range 0.10–0.22 MeV, using the cranking formulae [26] and leaving free the Harris parameters and the quasiparticle alignment. The alignments of bands 2 and 3 show a similar behavior with an indication of the first $\nu i_{13/2}$ band crossing (called AB) at around 0.28 MeV. This value is close to the AB crossing frequency observed in the neighboring even-even nucleus ^{164}Er [18] and in many nuclei in this mass region; however it is worth noting that an unexpected large value, $\hbar\omega_c = 0.35$ MeV, was recently observed in the other neighboring even-even nucleus ^{162}Dy which is not yet completely understood [3]. A different pattern presents the alignment of band 4 which remains almost constant over the whole range of rotational frequencies indicating a clear delay in the AB band crossing with respect to bands 2 and 3. This effect has been observed systematically in the $\pi 1/2^-[541]$ structures [21,27]. The value of $\hbar\omega_c \geq 0.35$ MeV obtained for band 4 follows the systematics for the $N = 96$ isotones for which $\hbar\omega_c$ increases when Z decreases [21].

Table 1. Configurations observed in ^{164}Ho.

Band	Proton	Neutron	K^π	Σ	Bandhead energy (keV)
1	$7/2^-[523]$	$5/2^-[523]$	6^+	0	191.1
2	$7/2^-[523]$	$5/2^+[642]$	6^-	1	139.9
3	$7/2^-[523]$	$3/2^-[521]$	5^+	1	342.7
4	$7/2^-[523]$	$5/2^-[523]$	1^+	1	0.0
5	$7/2^-[523]$	$5/2^+[642]$	1^-	0	193.3

The lower states of bands 3 and 4 are strongly connected through $\Delta I = 1$, $E1$ transitions which compete with the $E2$ intraband transitions. The $B(E1)$ strengths of these interband lines were extracted from the $E2/E1$ branching ratios and using the rotational model to evaluate the $B(E2)$ with a quadrupole moment of 7.3 eb (the average of the experimental values for the neighboring even-even nuclei ^{162}Dy and ^{164}Er [28]). The $B(E1)$ values obtained for the 127.4, 158.4, and 181.7 keV $\pi 1/2^-[541] \rightarrow \pi 1/2^+[411]$ transitions fall around 2×10^{-3} e^2fm^2 as in the ^{165}Tm case [21]. These enhanced $E1$ transitions are a well-known feature of the decays between the $\pi 1/2^+[411]$ and the $\pi 1/2^-[541]$ structures and have been interpreted in terms of particle-vibrational octupole couplings [29,30].

4.2 The ^{164}Ho nucleus

The configurations of bands in ^{164}Ho correspond to the coupling of the low-lying single-particle states observed in the odd-A neighboring nuclei of ^{164}Ho, the $7/2^-[523]$ orbital for the proton and the $5/2^-[523]$, $5/2^+[642]$, and $3/2^-[521]$ orbitals for the neutron. For each pair of proton and neutron orbitals there are two possible couplings, the low-K, $K_< = |\Omega_p - \Omega_n|$, and the high-$K$, $K_> = \Omega_p + \Omega_n$, couplings. If the intrinsic spins are coupled parallel ($\Sigma = \pm 1$) or antiparallel ($\Sigma = 0$), the corresponding states are placed lower or higher in energy, respectively, according to the Gallagher-Moszkowski (GM) coupling rules [31]. These two $K_{><}$ bands constitute the so-called GM doublet. Two GM doublets were identified in ^{164}Ho corresponding to the $\pi 7/2^-[523] \otimes \nu 5/2^-[523]$ (bands 1 and 4) and the $\pi 7/2^-[523] \otimes \nu 5/2^+[642]$ (bands 2 and 5) configurations. A list of the couplings established in ^{164}Ho is shown in table 1. The level energies of the bands for the low-K and high-K couplings constitute an important tool in the knowledge of the p-n interaction. The energy of a state of angular momentum I in a rotational band of an odd-odd nucleus in the case $K \neq 0$, neglecting the nondiagonal contributions of the Coriolis and of the p-n residual interaction, can be written as [32]

$$E_{IK} = E_p + E_n + \frac{\hbar^2}{2J}\left[I(I+1) - K^2\right] + E^K_{\rm int}\,,$$

where $E^K_{\rm int}$ is the diagonal part of the p-n interaction. The energy separation between the two $K_{><}$ members of the GM doublet, appropriately corrected for the zero-point rotational energy, is called the GM splitting energy

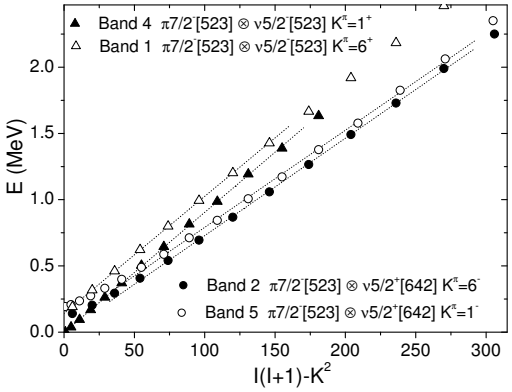

Fig. 9. Experimental level energies of GM doublets of ^{164}Ho and the linear fits (dotted lines) according to the rotational formula.

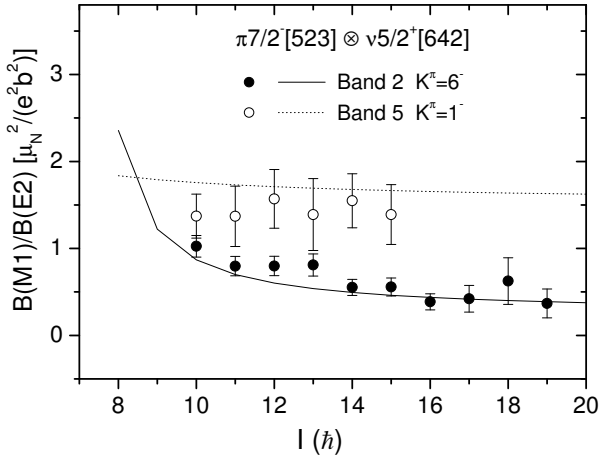

Fig. 10. Experimental and predicted $B(M1)/B(E2)$ values for bands 2 and 5 of ^{164}Ho. The parameters used in the calculations of the theoretical $B(M1)/B(E2)$ ratios are $Q_0 = 7.5$ *eb*, $g_R = 0.3$, $g_{\Omega_p} = 1.33$, $g_{\Omega_n} = -0.308$, $i_p = 0.5$ $\hbar$, and $i_n = 2.3$ $\hbar$.

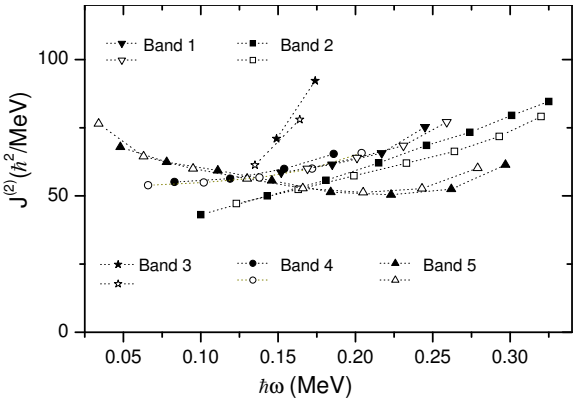

Fig. 11. Dynamical moments of inertia of bands of ^{164}Ho as a function of the rotational frequency. Filled and open symbols correspond to the $\alpha = 0$ and $\alpha = 1$ signatures, respectively.

and is defined by the expression: $\Delta E_{\rm GM} = E_{\rm int}^{K<} - E_{\rm int}^{K>}$. This GM splitting can be observed in fig. 9 where the level energies for the two GM doublets observed in ^{164}Ho, bands 1 and 4 and bands 2 and 5, are plotted as a function of $I(I+1) - K^2$. Linear fits of data for each rotational band according to the expression given above for E_{IK} were performed to obtain the empirical $\Delta E_{\rm GM}$ in the strong-coupling limit [32]. These fits are shown as dotted lines in fig. 9. The fits for both members of the $\pi 7/2^-[523] \otimes \nu 5/2^-[523]$ GM doublet performed up to $E \approx 1.5$ MeV, gave almost the same inertia parameter $\hbar^2/2J \approx 9$ keV and from the difference between the ordinates a $\Delta E_{\rm GM} = -145$ keV value was obtained. For the $\pi 7/2^-[523] \otimes \nu 5/2^+[642]$ GM doublet the data were fitted in the energy range 0.4–2.1 MeV, values of 7.3 keV were obtained for the inertia parameter of each band and the difference between the ordinates produced $\Delta E_{\rm GM} = 65$ keV. The $\Delta E_{\rm GM}$ value for the $\pi 7/2^-[523] \otimes \nu 5/2^-[523]$ GM doublet is in very good agreement with the one obtained in the fit of a more reduced data set and with the theoretical predictions reported in refs. [32,33]. From the inspection of fig. 9 a difference between both GM doublets emerges specially in the low-energy range, where the level sequences of the $\pi 7/2^-[523] \otimes \nu 5/2^+[642]$ GM doublet appear quite distorted consistent with the presence of the $\nu i_{13/2}$ for which the Coriolis effects are more important.

The analysis of other properties of the bands, such as the $B(M1)/B(E2)$ ratios and the evolution of the dynamical moments of inertia, which are sensitive to their intrinsic structures, confirmed the configuration assignments of the bands. The experimental in-band $B(M1; I \to I-1)/B(E2; I \to I-2)$ ratios were computed from the γ branching ratios assuming pure dipole character for the $\Delta I = 1$ transitions and compared with the values predicted by the geometrical model [34]. Figure 10 shows the measured $B(M1)/B(E2)$ ratios for the $\pi 7/2^-[523] \otimes \nu 5/2^+[642]$ $K^\pi = 1^-$ and $K^\pi = 6^-$ structures and the theoretical predictions which are consistent with the data. The experimental $B(M1)/B(E2)$ ratios for the $K^\pi = 1^-$ band are about 50–100% higher than those corresponding to the $K^\pi = 6^-$ band. This enhancement effect of the $M1$ transitions is explained by the fact that the antiparallel coupling of intrinsic spins corresponds to the parallel coupling of the spin magnetic dipole moments, which are therefore added constructively, as already reported in the ^{164}Tm case [35].

The first $\nu i_{13/2}$ band crossing (AB) (assumed to occur at $\hbar\omega_c \approx 0.28$ MeV in this mass region) can be checked in the plot of the dynamical moment of inertia *versus* rotational frequency. In fig. 11 a clear delay in the band crossing is observed in bands 2 ($\hbar\omega_c \geq 0.32$ MeV) and 5 ($\hbar\omega_c \geq 0.30$ MeV), due to blocking, compatible with the structures of these bands which contain the $\nu i_{13/2}$ as an active particle in their configurations. For bands 1, 3, and 4 the observed rotational frequency was not high enough to extract conclusions from the band crossings (fig. 11).

5 Conclusions

The ^{163,164}Ho nuclei were populated using the incomplete-fusion ^{160}Gd(^{11}B, αxn) reaction. For the ^{163}Ho the known

bands were extended with respect to previous works, and the 3qp $\pi 7/2^-[523] \otimes \nu 5/2^+[642] \otimes \nu 5/2^-[523]$ $K^\pi = 17/2^+$ band was observed together with its decay into the $\pi 7/2^-[523]$ band via $E1$ transitions. From the present data and the previous knowledge of ^{164}Ho five rotational bands were constructed for this nucleus from their bandheads and their decays were established. The level energies were fitted according to the rotational formula for the $\pi 7/2^-[523] \otimes \nu 5/2^-[523]$ and $\pi 7/2^-[523] \otimes \nu 5/2^+[642]$ GM doublets and empirical GM splitting energies were extracted.

References

1. D. Bazzacco, in *Proceedings of the International Conference on Nuclear Structure at High Angular Momentum, Ottawa, 1992*, Report No. AECL 10613, Vol. **2** (1992) p. 376.
2. M.A. Cardona *et al.*, Phys. Rev. C **66**, 044308 (2002).
3. A. Jungclaus *et al.*, Phys. Rev. C **66**, 014312 (2002).
4. G.D. Dracoulis *et al.*, J. Phys. G **23**, 1191 (1997).
5. L. Funke *et al.*, Nucl. Phys. A **190**, 576 (1972).
6. J.D. Panar *et al.*, Can. J. Phys. **55**, 1657 (1977).
7. D.G. Burke *et al.*, Nucl. Phys. A **359**, 36 (1981).
8. H.D. Jones, R.K. Sheline, Nucl. Phys. A **150**, 497 (1970).
9. J.-S. Tsai *et al.*, Z. Phys. A **322**, 295 (1985).
10. K. Walther, L. Funke, Annu. Rep. (Rossendorf) ZfK-243, 58 (1972).
11. K.D. Schilling *et al.*, Nucl. Phys. A **299**, 189 (1978).
12. B.P. Pathak, S.K. Mukherjee, Nucl. Phys. A **160**, 618 (1971).
13. L.K. Peker, Nucl. Data Sheets **65**, 439 (1992).
14. S.J. Mannanal *et al.*, Nucl. Phys. A **582**, 141 (1995).
15. C.M. Baglin, Nucl. Data Sheets **90**, 431 (2000).
16. A. Gavron, Phys. Rev. C **21**, 230 (1980).
17. B. Singh, A.R. Farhan, Nucl. Data Sheets **89**, 1 (2000).
18. B. Singh, Nucl. Data Sheets **93**, 243 (2001).
19. R.G. Helmer, C.W. Reich, Nucl. Data Sheets **87**, 317 (1999).
20. K.E.G. Löbner, Phys. Lett. B **26**, 369 (1968); in *The Electromagnetic Interaction in Nuclear Spectroscopy*, edited by W.D. Hamilton (North-Holland, Amsterdam, 1975) p. 141.
21. H.J. Jensen *et al.*, Nucl. Phys. A **695**, 3 (2001).
22. P.M. Walker, J. Phys. G **16**, L233 (1990).
23. P.M. Walker *et al.*, Phys. Lett. B **408**, 42 (1997).
24. Ts. Venkova *et al.*, Z. Phys. A **344**, 417 (1993).
25. A. Charvet *et al.*, Nucl. Phys. A **213**, 117 (1973).
26. R. Bengtsson, S. Frauendorf, Nucl. Phys. A **327**, 139 (1979).
27. H.J. Jensen *et al.*, Z. Phys. A **359**, 127 (1997).
28. S. Raman *et al.*, At. Data Nucl. Data Tables **36**, 1 (1987).
29. I. Hamamoto *et al.*, Phys. Lett. B **226**, 17 (1989).
30. G.B. Hagemann *et al.*, Phys. Rev. C **47**, 2008 (1993).
31. C.J. Gallagher jr., S.A. Moszkowski, Phys. Rev. **111**, 1282 (1958).
32. A.K. Jain *et al.*, Rev. Mod. Phys. **70**, 843 (1998).
33. J.P. Boisson *et al.*, Phys. Rep. **26**, 99 (1976).
34. F. Dönau, S. Frauendorf, in *Proceedings of the Conference on High Angular Momentum Properties of Nuclei, Oak Ridge, USA, 1982*, edited by N. Johnson (Harwood Academic, Chur, Switzerland, 1982) p. 143.
35. W. Reviol *et al.*, Phys. Rev. C **59**, 1351 (1999).